

# The 1/2-Complex Bruno Function and the Yoccoz Function: A Numerical Study of the Marmi-Moussa-Yoccoz Conjecture

Timoteo Carletti

## CONTENTS

- 1. Introduction
- 2. The 1/2-Complex Bruno Functions
- 3. The Yoccoz Function
- 4. The Littlewood-Paley Theory
- 5. Presentation of Numerical Results
- Appendix A. Numerical Considerations
- References

---

We study the 1/2-Complex Bruno function and we produce an algorithm to evaluate it numerically, giving a characterization of the monoid  $\hat{\mathcal{M}} = \mathcal{M}_T \cup \mathcal{M}_S$ . We use this algorithm to test the Marmi-Moussa-Yoccoz Conjecture about the Holder continuity of the function  $z \mapsto -i\mathbf{B}(z) + \log U(e^{2\pi iz})$  on  $\{z \in \mathbb{C} : \Im z \geq 0\}$ , where  $\mathbf{B}$  is the 1/2-complex Bruno function and  $U$  is the Yoccoz function. We give a positive answer to an explicit question of S. Marmi et al [Marmi et al. 01].

---

## 1. INTRODUCTION

The *real Bruno functions* are arithmetical functions  $B_\alpha : \mathbb{R} \setminus \mathbb{Q} \rightarrow \mathbb{R}_+ \cup \{+\infty\}$ ,  $\alpha \in [1/2, 1]$  which characterize numbers by their rate of approximation by rationals. They have been introduced by J.-C. Yoccoz [Yoccoz 95] (cases  $\alpha = 1/2$  and  $\alpha = 1$ ) and then studied in a more general context in [Marmi et al. 97].

For their relationship with arithmetical properties of real numbers, Bruno's functions enter in a huge number of dynamical system problems involving small divisors, for instance in the problem of the *stability of a fixed point* of a holomorphic diffeomorphism of a complex variable (the so-called *Schröder-Siegel* problem) [Yoccoz 95], in the *Schröder-Siegel* problem in the *Gevrey* setting in one complex variable [Carletti and Marmi 00] or several variables [Carletti 03], and in some *local conjugacy* problems: *semistandard map* [Marmi 90, Davie 94], *analytic circle diffeomorphisms* [Yoccoz 02], and some *analytic area-preserving annulus maps* including the *Standard map* and some of its generalizations [Berretti and Gentile 01].

Let us now concentrate on the 1/2-Bruno function.<sup>1</sup>  $B_{1/2}$  is  $\mathbb{Z}$ -periodic, even, (for this reason it is also called

---

<sup>1</sup>From [Marmi et al. 97], we know that the difference of any two Bruno's functions is in  $L^\infty(\mathbb{R})$ .

2000 AMS Subject Classification: Primary 37F50, 42B25

Keywords: Complex Bruno Function, Yoccoz Function, linearization of quadratic polynomial, Littlewood-Paley dyadic decomposition, continued fraction, Farey series

even Bruno’s function), and verifies the functional equation:

$$B_{1/2}(x) = -\log x + xB_{1/2}(x^{-1}) \quad x \in (0, 1/2). \quad (1-1)$$

The set  $\mathcal{B} = \{x \in \mathbb{R} : B_{1/2}(x) < +\infty\}$  is called the set of Bruno’s numbers: By (1-1), it follows that  $\mathcal{B}$  is invariant under the action of the modular group

$$GL(2, \mathbb{Z}) = \left\{ \begin{pmatrix} a & b \\ c & d \end{pmatrix} : a, b, c, d \in \mathbb{Z}, ad - bc = \pm 1 \right\}.$$

The Bruno function can be extended to rational numbers by setting  $B_{1/2}(x) = +\infty$  when  $x \in \mathbb{Q}$ .

Using the continued fraction algorithm, one can solve (1-1) to obtain:

$$B_{1/2}(x) = \sum_{k \geq 0} \beta_{k-1}(x) \log x_k^{-1}, \quad (1-2)$$

where  $x_0 = x$ ,  $x_k = A_{1/2}(x_{k-1})$ ,  $\beta_{-1} = 1$ ,  $\beta_k = \prod_{j=0}^k x_j$ , and  $A_{1/2}$  is the nearest integer continued fraction map. In Section 2.1, we will give a brief account of useful facts concerning continued fractions.

In [Marmi et al. 01], the complex Bruno function has been introduced;<sup>2</sup> more precisely, the authors defined an analytic map  $\mathbf{B} : \mathbb{H}^+ \rightarrow \mathbb{H}^+$ , where  $\mathbb{H}^+$  is the upper Poincaré half plane,  $\mathbb{Z}$ -periodic, which verifies a functional equation similar to the one for the 1-Bruno function. The boundary behavior of  $\mathbf{B}$  is given by (see Theorem 5.19 and Section 5.2.9 of [Marmi et al. 01]):

1. Let  $H > 0$ , then the imaginary part of  $\mathbf{B}(z + \omega)$  tends to  $B_{1/2}(\omega)$  when  $\Im z \rightarrow 0$  and  $z \in \{\zeta \in \mathbb{H}^+ : \Im \zeta \geq |\Re \zeta|^H\}$ , whenever  $\omega \in \mathcal{B}$ ;
2.  $\Re \mathbf{B}(z)$  is bounded on  $\mathbb{H}^+$ , its trace on  $\partial \mathbb{H}^+$  is continuous at irrational points, and it has a jump of  $\pi/q$  for  $\Re z = p/q \in \mathbb{Q}$ .

In Section 2, we introduce an explicit formula for the 1/2-complex Bruno function which corrects a small error in Section A.4.4, page 836, and gives more details than Appendix A.4 of [Marmi et al. 01]. We will also give an algorithm to compute it numerically.

<sup>2</sup>Following the notation introduced for the real Bruno functions, we should call this complex extension the 1-complex Bruno function. In fact, we will see at the end of Section 2 that it is constructed “following” the Gauss continued fraction algorithm. In this way, we could also distinguish it from the 1/2-complex Bruno function that we will introduce in Section 2 “following” the nearest integer continued fraction algorithm.

### 1.1 The Yoccoz Function

We already observed that the function  $B_{1/2}$  is related to the stability problem of a fixed point of an analytic diffeomorphism of  $\mathbb{C}$ ; in the rest of this section, we will show this relation by describing the Yoccoz result ([Yoccoz 95], Chapter II). Let  $\lambda \in \mathbb{C}^*$  and let us consider the quadratic polynomial  $P_\lambda(z) = \lambda z(1 - z)$ . The origin is a fixed point and we are interested in studying its stability. If  $|\lambda| < 1$  (hyperbolic case), then it follows from the results of Poincaré and Koenigs that the origin is stable, whereas if  $\lambda = e^{2\pi ip/q}$  (parabolic case), the origin is not stable.

Let now consider  $\lambda \in \mathbb{D}^*$  and let  $H_\lambda(z)$  be the conformal map which locally linearizes  $P_\lambda$  (its existence is guaranteed by the Poincaré-Koenigs results):

$$P_\lambda \circ H_\lambda = H_\lambda \circ R_\lambda, \quad (1-3)$$

where  $R_\lambda(z) = \lambda z$ , and let us denote by  $r_2(\lambda)$  the radius of convergence of  $H_\lambda$ .

One can prove that  $H_\lambda$  can be analytically continued to a larger set, the basin of attraction of 0:  $\{z \in \mathbb{C} : P_\lambda^{\circ n}(z) \rightarrow 0, n \rightarrow +\infty\}$ , but not to the whole of  $\mathbb{C}$ , and it has a unique singular point on its circle of convergence  $\mathbb{D}_{r_2(\lambda)}$ , which will be denoted by  $U(\lambda) \in \mathbb{C}$ . The function  $U : \mathbb{D}^* \rightarrow \mathbb{C}$  is called the Yoccoz function.

Yoccoz proved that  $U$  has an analytic bounded extension to  $\mathbb{D}$  and moreover it can be obtained as a limit of polynomials  $U_n(\lambda) = \lambda^{-n} P_\lambda^{\circ n}(z_{crit})$ , uniformly over compact subsets of  $\mathbb{D}$ , where  $z_{crit} = 1/2$  is the critical point of the quadratic polynomial. Since this extension is not identically zero, by a classical result of Fatou, the Yoccoz function has radial limits almost everywhere, and the set  $\lambda_0 \in S^1$  for which  $\limsup_{\lambda \rightarrow \lambda_0} U(\lambda) = 0$  has zero measure. Moreover, Yoccoz proved that for all  $\lambda_0 \in S^1$ , the module of  $U(\lambda)$  admits a nontangential limit in  $\lambda_0$  which equals  $r_2(\lambda_0)$ : the radius of convergence of  $H_{\lambda_0}$ . This means that the quadratic polynomial is linearizable ( $r_2(\lambda_0) = |U(\lambda_0)| > 0$ ) for a full measure set of  $\lambda_0 \in S^1$ , but the proof doesn’t give any information on this set.

When  $|\lambda| = 1$  and  $\lambda$  is not a root of the unity, assuming  $\lambda = e^{2\pi i \omega}$ , for some irrational  $|\omega| < 1/2$ , Yoccoz proved ([Yoccoz 95], Theorem 1.8, Chapter II) that  $P_\lambda(z)$  is linearizable if and only if  $\omega \in \mathcal{B}_{1/2}$ ; moreover, there exists a constant  $C_1$ , and for all  $\epsilon > 0$  a constant  $C(\epsilon)$  such that for all  $\omega \in \mathcal{B}_{1/2}$ ,

$$C_1 \leq \log r_2(e^{2\pi i \omega}) + B_{1/2}(\omega) \leq C(\epsilon) + \epsilon B_{1/2}(\omega).$$

We are then interested in studying the function  $\omega \mapsto \log |U(e^{2\pi i \omega})| + B_{1/2}(\omega)$  and some “natural” questions arise ([Yoccoz 95] Section 3.2, page 72):

**Conjecture 1.1. (Yoccoz Conjecture.)** *Is the function  $\omega \mapsto \log |U(e^{2\pi i\omega})| + B_{1/2}(\omega)$  bounded for  $\omega \in \mathbb{R}$ ?*

Motivated by numerical results of [Marmi 90] and by some analytic properties of the real Bruno function (see Remark 1.3 and [Marmi et al. 97]), it has been conjectured that:

**Conjecture 1.2. (Marmi-Moussa-Yoccoz Conjecture.)** *The function, defined on the set of Bruno number,  $\omega \mapsto \log |U(e^{2\pi i\omega})| + B_{1/2}(\omega)$ , extends to a 1/2-Hölder continuous function on  $\mathbb{R}$ .*

**Remark 1.3. (Why 1/2-Hölder?)** In [Marmi et al. 97], the authors proved a “stability result” for  $B_{1/2}$  (Section 4, page 285). Let us rewrite the functional equation for the 1/2-Bruno function as follow:

$$[B_{1/2}(x) - xB_{1/2}(x^{-1})] = -\log x,$$

if we add to the r.h.s. a “regular term”  $f$ , say  $\eta$ -Hölder continuous, and we call  $B_f$  the solution of:

$$[B_f(x) - xB_f(x^{-1})] = -\log x + f(x),$$

then  $B_{1/2} - B_f$  is 1/2-Hölder continuous if  $f$  is at least 1/2-Hölder. Hence, if we prove<sup>3</sup> that the function  $\omega \mapsto [\log |U(e^{2\pi i\omega})| - \omega \log |U(e^{2\pi i\omega^{-1}})|] - \log \omega$  is Hölder continuous with exponent  $\eta \geq 1/2$ , for  $\omega \in [0, 1/2]$ , then Conjecture 1.2 holds.

X. Buff and A. Cheritat [Buff and Cheritat 03] proved the Yoccoz conjecture, and in the very recent preprint [Buff and Cheritat 04], they also proved continuity. We will be interested in the following conjecture, equivalent to the one of Marmi-Moussa-Yoccoz:

**Conjecture 1.4.** *The analytic function, defined on the upper Poincaré half plane,  $z \mapsto \mathcal{H}(z) = \log U(e^{2\pi iz}) - i\mathbf{B}(z)$ , extends to a 1/2-Hölder continuous function on  $\mathbb{H}^+$ .*

The aim of this paper is two-fold: first, to give more insight into the 1/2-complex Bruno function and second to make a first step toward the understanding of Conjecture 1.4. Our numerical results allow us to conclude

<sup>3</sup>Transform a function according to  $\psi(x) \mapsto \psi(x) - x\psi(1/x)$  to “reduce the strength of singularities” is the main idea of the *Modular Smoothing*. We refer to [Buric et al. 90] where the authors describe the method and apply it to the critical function of the semistandard map.

that  $\mathcal{H}$  is  $\eta$ -Hölder continuous and we obtain an estimate of the Hölder exponent  $\eta = 0.498 \pm 0.004$ . This gives us good numerical evidence that the Marmi-Moussa-Yoccoz conjecture should be true.

The paper is organized as follows: In Section 2, we introduce the 1/2-complex Bruno function and some results from number theory (approximations of rationals by rationals) to obtain an algorithm to compute the complex Bruno function. In Section 3, we explain how to calculate the Yoccoz function and then, after a brief introduction of the Littlewood-Paley Theory in Section 4, used to test the Hölder continuity, we present our results in Section 5. Appendix 5.2 collects some considerations related to technical aspects of our numerical test.

## 2. THE 1/2-COMPLEX BRUNO FUNCTIONS

The aim of this section is to introduce, starting from Appendix A.4 of [Marmi et al. 01], a complex extension of the 1/2-real Bruno function and to give an algorithm to compute it numerically.

Let us consider  $f \in L^2([0, 1/2])$ , extended: 1-periodic,  $f(x+1) = f(x)$  for all  $x \in \mathbb{R}$ , and even  $f(x) = f(-x)$  for all  $x \in [-1/2, 0]$ , and then let us introduce the operator  $T$  acting on such  $f$  by

$$Tf(x) = xf\left(\frac{1}{x}\right); \tag{2-1}$$

we remark that the functional equation (1-1) can be rewritten as

$$(1 - T)B_{1/2}(x) = -\log x \quad \forall x \in (0, 1/2). \tag{2-2}$$

Let  $(T_m)_{m \geq 2}$  be the operators defined by

$$(T_m f)(x) = \begin{cases} xf\left(\frac{1}{x} - m\right) & x \in \left(\frac{1}{m+1/2}, \frac{1}{m}\right] \text{ branch } m^+ \\ xf\left(m - \frac{1}{x}\right) & x \in \left(\frac{1}{m}, \frac{1}{m-1/2}\right] \text{ branch } m^- \\ 0 & \text{otherwise;} \end{cases} \tag{2-3}$$

then using the periodicity and the evenness of  $f$ , we can rewrite (2-1) as follows:

$$Tf(x) = \sum_{m \geq 2} \left\{ xf\left(\frac{1}{x} - m\right) + xf\left(m + 1 - \frac{1}{x}\right) \right\}. \tag{2-4}$$

To introduce the 1/2-complex Bruno function, we have to extend (2-4) to complex analytic functions; this is done [Marmi et al. 01] by considering the complex vector space of holomorphic functions in  $\mathbb{C} \setminus [0, 1/2]$ , vanishing at infinity:  $\mathcal{O}^1(\mathbb{C} \setminus [0, 1/2])$  (which is isomorphic

to the space of hyperfunctions with support contained in  $[0, 1/2]$ . So, let  $\varphi$  be the Hilbert transform of  $f$ :

$$\varphi(z) = \frac{1}{\pi} \int_0^{1/2} \frac{f(x)}{x - z} dx;$$

then starting from (2-4), we define the action of  $T$  on  $\varphi$  as follows:

$$T\varphi(z) = \sum_{m \geq 2} L_{g(m)}(1 + L_\sigma)\varphi(z), \quad (2-5)$$

where  $g(m) = \begin{pmatrix} 0 & 1 \\ 1 & m \end{pmatrix}$ ,  $\sigma = \begin{pmatrix} -1 & 1 \\ 0 & 1 \end{pmatrix}$  and  $L_{\begin{pmatrix} a & b \\ c & d \end{pmatrix}}$  acts on  $\mathcal{O}^1(\mathbb{C} \setminus [0, 1/2])$  by

$$L_{\begin{pmatrix} a & b \\ c & d \end{pmatrix}}\varphi(z) = (a - cz) \left[ \varphi\left(\frac{dz - b}{a - cz}\right) - \varphi\left(-\frac{d}{c}\right) \right] - \frac{ad - bc}{c} \varphi'\left(-\frac{d}{c}\right). \quad (2-6)$$

In the spirit of (2-2), we want to consider  $(1 - T)^{-1}$  acting on some  $\varphi \in \mathcal{O}^1(\mathbb{C} \setminus [0, 1/2])$ , and to obtain a  $\mathbb{Z}$ -periodic, “even function,”<sup>4</sup> we will consider:

$$\sum_{n \in \mathbb{Z}} \left[ (1 + L_\sigma)(1 - T)^{-1} \right] \varphi(z - n). \quad (2-7)$$

Let us introduce the operator  $\hat{T}$  defined by  $(1 + L_\sigma)T = \hat{T}(1 + L_\sigma)$ , then from (2-5) and the relation,  $(1 - T)^{-1} = \sum_{r \geq 0} T^r$ , we can expand  $(1 - \hat{T})^{-1}$  in terms of matrices  $g(m)$  and  $\sigma$ , to obtain a sum of matrices of the form  $\epsilon_0 g(m_1) \dots \epsilon_{r-1} g(m_r)$ , where  $r \geq 1$ ,  $m_i \geq 2$ , and  $\epsilon_{i-1} \in \{1, \sigma\}$ , for  $1 \leq i \leq r$ .

Let us set  $\mathcal{M}^{(0)} = \{1\}$  and for  $r \geq 1$ :

$$\hat{\mathcal{M}}^{(r)} = \left\{ g \in GL(2, \mathbb{Z}) : \exists \epsilon_0, \dots, \epsilon_{r-1} \in \{1, \sigma\}, m_1, \dots, m_r \geq 2 : g = \epsilon_0 g(m_1) \dots \epsilon_{r-1} g(m_r) \right\}, \quad (2-8)$$

and finally  $\hat{\mathcal{M}} = \cup_{r \geq 0} \hat{\mathcal{M}}^{(r)}$ : the *1/2-Monoid* (we left to Section 2.3 a more detailed discussion of this monoid and the reason for its name).

It remains to specify the “good”  $\varphi \in \mathcal{O}^1(\mathbb{C} \setminus [0, 1/2])$  to apply (2-7), to have the desired properties for  $\mathbf{B}$ . This is done by considering the Hilbert transform of the logarithm restricted to  $(0, 1/2]$ , namely,

$$\begin{aligned} \varphi_{1/2}(z) &= \frac{1}{\pi} \int_0^{1/2} \frac{-\log x}{x - z} dx \\ &= -\frac{1}{\pi} Li_2\left(\frac{1}{2z}\right) + \frac{1}{\pi} \log 2 \log\left(1 - \frac{1}{2z}\right), \end{aligned} \quad (2-9)$$

<sup>4</sup>Here and in the following, by even complex function, we will mean even w.r.t.  $\Re z \rightarrow -\Re z$ .

where  $Li_2(z)$  is the *dilogarithm* function [Oesterlé 93]: the analytic continuation of  $\sum_{n \geq 1} z^n n^{-2}$ , to  $\mathbb{C} \setminus [1, +\infty)$ . We are now able to define the *1/2-complex Bruno function* to be

$$\mathbf{B}(z) = \sum_{n \in \mathbb{Z}} \left[ \sum_{g \in \mathcal{M}} L_g(1 + L_\sigma) \right] \varphi_{1/2}(z - n). \quad (2-10)$$

This formula defines<sup>5</sup> a holomorphic function, defined in  $\mathbb{H}^+$ ,  $\mathbb{Z}$ -periodic, such that

$$\Im \mathbf{B}(x + iy) = \Im \mathbf{B}(-x + iy)$$

and

$$\Re \mathbf{B}(x + iy) = -\Re \mathbf{B}(-x + iy),$$

for all  $y > 0$  and  $x \in [0, 1/2]$ .

**Remark 2.1.** The *1/2-complex Bruno function* is 1-periodic and so we can consider its Fourier series:  $\mathbf{B}(z) = \sum_{l \in \mathbb{Z}} \hat{b}_l e^{2\pi i l z}$ . Introducing the variable  $w = e^{2\pi i z}$ , the Bruno function is mapped into an analytic function,  $\tilde{\mathbf{B}}(w)$ , defined in  $\mathbb{D}^*$ , which can be extended by continuity to  $\mathbb{D}$ . Then its Taylor series at the origin is  $\tilde{\mathbf{B}}(w) = \sum_{l \in \mathbb{N}} \hat{b}_l w^l$ , hence Fourier coefficients of  $\mathbf{B}(z)$  corresponding to negative modes are all identically zero. Moreover, because of the parity properties of  $\Re \mathbf{B}$  and  $\Im \mathbf{B}$ , its Fourier coefficients are all purely imaginary; in fact,

$$\begin{aligned} \hat{b}_l &= 2i \int_0^{1/2} [-\sin(2\pi l x) \Re \mathbf{B}(x + it) \\ &\quad + \cos(2\pi l x) \Im \mathbf{B}(x + it)] dx. \end{aligned}$$

The goal of the next sections will be to express (2-10) in terms of a sum over a class of rational numbers in such a way we could give (Section 2.4) an algorithm to compute it. This will be accomplished thanks to a new characterization (Section 2.3) of the *1/2-Monoid*  $\hat{\mathcal{M}}$ , after having introduced some results from number theory (Sections 2.1 and 2.2).

### 2.1 Continued Fraction

We consider the so-called *nearest integer continued fraction* algorithm.<sup>6</sup> We state here some basic facts we will need in the following and we refer to [Hardy and Wright

<sup>5</sup>This claim can be obtained by slight modification of the proof given in [Marmi et al. 01] for the 1-Complex Bruno function and we omit it, referring to [Marmi et al. 01] for any details.

<sup>6</sup>In [Nakada 80], a one parameter family of continued fraction developments has been introduced. The nearest integer continued fraction corresponds to the value 1/2 of the parameter, so we will also call it *1/2-continued fraction*.

79, Marmi et al. 97] for a more complete discussion. Let  $\|x\| = \min_{p \in \mathbb{Z}} \{x < 1/2 + p\}$ , then to each  $x \in \mathbb{R}$ , we associate a continued fraction as follows:

$$\begin{aligned} a_0 &= \|x\| \\ x_0 &= |x - a_0| \\ \varepsilon_0 &= \begin{cases} +1 & \text{iff } x \geq a_0 \\ -1 & \text{otherwise,} \end{cases} \end{aligned} \tag{2-11}$$

and then inductively for all  $n \geq 0$ , as long as  $x_n \neq 0$ ,

$$\begin{aligned} a_{n+1} &= \|x_n^{-1}\|, \\ x_{n+1} &= |x_n^{-1} - a_{n+1}| \equiv A_{1/2}(x_n), \\ \varepsilon_{n+1} &= \begin{cases} +1 & \text{iff } x_n^{-1} \geq a_{n+1} \\ -1 & \text{otherwise.} \end{cases} \end{aligned} \tag{2-12}$$

We will use the standard compact notation to denote the continued fraction  $x = [(a_0, \varepsilon_0), \dots, (a_n + \varepsilon_n x_n, \varepsilon_n)]$ . From the definition, it follows that  $x_n > 2$  and so  $a_n \geq 2$ .

**Remark 2.2. (Standard form for finite continued fraction.)**

Let  $[(a_0, \varepsilon_0), \dots, (a_{\bar{n}}, \varepsilon_{\bar{n}})]$  be a finite continued fraction of length  $\bar{n}$ . Then, whenever  $a_{\bar{n}} = 2$ , we must also have  $\varepsilon_{\bar{n}-1} = +1$ , namely  $[(a_0, \varepsilon_0), \dots, (a_{\bar{n}-1}, -1), (2, +1)]$  represents the same rational number that  $[(a_0, \varepsilon_0), \dots, (a_{\bar{n}-1} - 1, +1), (2, +1)]$ . Moreover, a finite continued fraction cannot contain a couple  $(a_l, \varepsilon_l) = (2, -1)$  for any  $l \leq \bar{n}$ .

We recall, without proof, some known results:

- the continued fraction algorithm stops if and only if  $x \in \mathbb{R} \setminus \mathbb{Q}$  (this correspondence is bijective up to the standard convention of Remark 2.2);
- for any positive integer  $n$  (or smaller than the length of the finite continued fraction) the  $n^{\text{th}}$  convergent is defined by

$$\frac{p_n}{q_n} = [(a_0, \varepsilon_0), \dots, (a_n, \varepsilon_n)]; \tag{2-13}$$

one can prove that  $p_n$  and  $q_n$  are recursively defined by

$$\begin{cases} p_n = a_n p_{n-1} + \varepsilon_{n-1} p_{n-2} \\ q_n = a_n q_{n-1} + \varepsilon_{n-1} q_{n-2}, \end{cases} \tag{2-14}$$

starting with  $p_{-1} = q_{-2} = 1, p_{-2} = q_{-1} = 0$ , and  $\varepsilon_{-1} = 1$ ;

- for all  $n$ , we have:  $q_n p_{n-1} - p_n q_{n-1} = (-1)^n \varepsilon_0 \dots \varepsilon_{n-1}$ .

**2.2 The Farey Series**

Let  $n \in \mathbb{N}^*$ ; the *Farey Series* [Hardy and Wright 79] of order  $n$  is the set of irreducible fractions in  $[0, 1]$  whose denominators do not exceed  $n$ :<sup>7</sup>

$$\mathcal{F}_n = \{p/q \in [0, 1] : (p, q) = 1 \text{ and } q \leq n\}. \tag{2-15}$$

The cardinality of  $\mathcal{F}_n$  is given by  $\Phi(n) = 1 + \sum_{l=2}^n \phi(l)$ , where  $\phi(n)$  is the Euler totient function and so this cardinality is asymptotic to  $3n^2/\pi^2$  for  $n$  large. The Farey Series is characterized by the following two properties [Hardy and Wright 79]:

**Theorem 2.3.** *Let  $n \geq 1$ . If  $p/q$  and  $p'/q'$  are two successive elements of  $\mathcal{F}_n$ , then  $qp' - q'p = 1$ .*

**Theorem 2.4.** *Let  $n \geq 1$ . If  $p'/q', p/q$ , and  $p''/q''$  are three successive elements (in this order) of  $\mathcal{F}_n$ , then:*

$$\frac{p}{q} = \frac{p' + p''}{q' + q''}.$$

Using an idea contained in the proof of Theorem 2.4 given in [Hardy and Wright 79], we construct an algorithm (easily implementable on a computer) which allows us to carry out for any  $n \geq 2$  the Farey Series of order  $n$ . Using Proposition 2.6, we will give a second algorithm to compute the Farey Series up to any given order  $n$ , using the continued fraction development.

**Proposition 2.5. (Construction of  $\mathcal{F}_n$ .)** *Let  $n \geq 2$ , then the elements of  $\mathcal{F}_n$ ,  $(p_i/q_i)_{1 \leq i \leq \phi(n)}$ , are recursively defined by*

$$\begin{cases} p_{i+1} = -p_{i-1} + r_i p_i \\ q_{i+1} = -q_{i-1} + r_i q_i, \end{cases} \tag{2-16}$$

where  $r_i = \lfloor (n + q_{i-1})/q_i \rfloor$ , starting with  $(p_1, q_1) = (0, 1)$ ,  $(p_2, q_2) = (1, n)$ , and  $(p_3, q_3) = (1, n - 1)$ .

*Proof:* Let  $p/q \in \mathcal{F}_n$ . Because  $p$  and  $q$  are relatively prime, we can always solve in  $\mathbb{Z}^2$  the linear Diophantine equation  $qP - pQ = 1$ : Let  $(P_0, Q_0)$  be a particular solution and let  $r$  be the integer such that  $n - q < Q_0 + r q \leq n$ , namely  $r = \lfloor (n - Q_0)/q \rfloor$ .

<sup>7</sup>This is different from the *Farey Tree* which is still a set of rational numbers in  $[0, 1]$  which can be constructed by induction starting with  $\hat{\mathcal{F}}_0 = \{0, 1\}$  and then defining the  $i$ -th element of  $\hat{\mathcal{F}}_n$ ,  $n \geq 1$ , by

$$\frac{\hat{p}_i^{(n)}}{\hat{q}_i^{(n)}} = \frac{\hat{p}_{i-1}^{(n-1)} + \hat{p}_i^{(n-1)}}{\hat{q}_{i-1}^{(n-1)} + \hat{q}_i^{(n-1)}}.$$

The Farey Tree of order  $n$  is clearly larger than the corresponding Farey Series and  $\text{card} \hat{\mathcal{F}}_n = 2^n + 1$ .

Let us define  $P_r = P_0 + rp$  and  $Q_r = Q_0 + rq$ ; then the following claims are trivial:  $(P_r, Q_r)$  is again a solution of the linear diophantine equation,  $(P_r, Q_r) = 1$  and  $0 < Q_r \leq n$ . So  $P_r/Q_r \in \mathcal{F}_n$ . Clearly,  $P_r/Q_r > p/q$  and we claim that it is the immediate successor of  $p/q$  in  $\mathcal{F}_n$ .

To obtain a constructive algorithm, we must solve the linear diophantine equation; this is achieved by considering the element which precedes  $p/q$  in  $\mathcal{F}_n$ : Let us denote it by  $p'/q'$ . A particular solution is then given by  $P_0 = -p'$ ,  $Q_0 = -q'$ ; from the previous result, the element following  $p/q$  is then given by  $P_r = -p' + rp$ ,  $Q_r = -q' + rq$ , where  $r = \lfloor (n + q')/q \rfloor$ .

To finish the algorithm, we need two starting elements of  $\mathcal{F}_n$  apart of  $0/1$ , but it is easy to realize that the first three elements of  $\mathcal{F}_n$  are  $0/1$ ,  $1/n$  and  $1/(n-1)$ , whenever  $n \geq 2$ . □

We are now able to give a second algorithm to construct the Farey Series of order  $n$ . Here is the idea: Given an irreducible fraction  $p/q \in (0, 1)$ , we compute its continued fraction development and then following two rules, *Truncate* and *Subtract one*, we obtain two new irreducible fractions in  $[0, 1]$  which will be the predecessor and the successor of  $p/q$  in  $\mathcal{F}_n$  with  $n = q$ .

**Proposition 2.6. (Construction of  $\mathcal{F}_n$ , 2nd version.)** *Let  $p/q \in (0, 1)$  and let  $p'/q' < p/q < p''/q''$  be three successive elements of  $\mathcal{F}_q$ . Assume  $p/q = [(a_0, \varepsilon_0), \dots, (a_{\bar{n}}, \varepsilon_{\bar{n}})]$  for some  $\bar{n} \geq 1$  and let us define the rational numbers  $p_T/q_T$  and  $p_S/q_S$  as follows:<sup>8</sup>*

$$\frac{p_T}{q_T} = [(a_0, \varepsilon_0), \dots, (a_{\bar{n}-1}, \varepsilon_{\bar{n}-1})] \quad (\text{Truncate}), \quad (2-17)$$

and

$$\frac{p_S}{q_S} = [(a_0, \varepsilon_0), \dots, (a_{\bar{n}} - 1, \varepsilon_{\bar{n}})] \quad (\text{Subtract one}). \quad (2-18)$$

Then if  $\varepsilon_0 \dots \varepsilon_{\bar{n}-1} = +1$ , we have

$$\begin{cases} p_T/q_T = p'/q', \text{ and, } p_S/q_S = p''/q'' & \text{if } \bar{n} \text{ is even} \\ p_T/q_T = p''/q'', \text{ and, } p_S/q_S = p'/q' & \text{if } \bar{n} \text{ is odd.} \end{cases} \quad (2-19)$$

Whereas if  $\varepsilon_0 \dots \varepsilon_{\bar{n}-1} = -1$ , we have the symmetric case, namely

$$\begin{cases} p_T/q_T = p''/q'', \text{ and, } p_S/q_S = p'/q' & \text{if } \bar{n} \text{ is even} \\ p_T/q_T = p'/q', \text{ and, } p_S/q_S = p''/q'' & \text{if } \bar{n} \text{ is odd.} \end{cases} \quad (2-20)$$

<sup>8</sup>If  $a_{\bar{n}} = 2$ , then  $\varepsilon_{\bar{n}-1} = +1$  by Remark 2.2, and  $p_S/q_S = [(a_0, \varepsilon_0), \dots, (a_{\bar{n}-1} + 1, +1)]$ .

*Proof:* By (2-14), (2-17), and (2-18), we have

$$\begin{cases} p_T &= a_{\bar{n}-1}p_{\bar{n}-2} + \varepsilon_{\bar{n}-2}p_{\bar{n}-3} \\ q_T &= a_{\bar{n}-1}q_{\bar{n}-2} + \varepsilon_{\bar{n}-2}q_{\bar{n}-3} \end{cases}$$

and

$$\begin{cases} p_S &= (a_{\bar{n}} - 1)p_{\bar{n}-1} + \varepsilon_{\bar{n}-1}p_{\bar{n}-2} \\ q_S &= (a_{\bar{n}} - 1)q_{\bar{n}-1} + \varepsilon_{\bar{n}-1}q_{\bar{n}-2}, \end{cases}$$

then,

$$\begin{aligned} \frac{p_T + p_S}{q_T + q_S} &= \\ \frac{a_{\bar{n}-1}p_{\bar{n}-2} + \varepsilon_{\bar{n}-2}p_{\bar{n}-3} + (a_{\bar{n}} - 1)p_{\bar{n}-1} + \varepsilon_{\bar{n}-1}p_{\bar{n}-2}}{a_{\bar{n}-1}q_{\bar{n}-2} + \varepsilon_{\bar{n}-2}q_{\bar{n}-3} + (a_{\bar{n}} - 1)q_{\bar{n}-1} + \varepsilon_{\bar{n}-1}q_{\bar{n}-2}} &= \\ = \frac{p_{\bar{n}}}{q_{\bar{n}}} = \frac{p}{q}, \end{aligned}$$

where we used the definition of  $p/q$  with its finite continued fraction of length  $\bar{n}$ . Finally,

$$\frac{p}{q} - \frac{p_T}{q_T} = \frac{p_{\bar{n}}q_{\bar{n}-1} - p_{\bar{n}-1}q_{\bar{n}}}{q_{\bar{n}}q_{\bar{n}-1}} = \frac{(-1)^{\bar{n}+1}\varepsilon_0 \dots \varepsilon_{\bar{n}-1}}{q_{\bar{n}}q_{\bar{n}-1}},$$

and similarly

$$\begin{aligned} \frac{p}{q} - \frac{p_S}{q_S} &= \frac{p_{\bar{n}}(q_{\bar{n}} - q_{\bar{n}-1}) - (p_{\bar{n}} - p_{\bar{n}-1})q_{\bar{n}}}{q_{\bar{n}}q_S} \\ &= \frac{(-1)^{\bar{n}}\varepsilon_0 \dots \varepsilon_{\bar{n}-1}}{q_{\bar{n}}q_S}, \end{aligned}$$

from which the proof follows easily. □

### 2.3 The 1/2-Monoid

In this paragraph, we will study the monoid  $\hat{\mathcal{M}}$  of  $GL(2, \mathbb{Z})$ , introduced in (2-8) and used in the construction of the 1/2-Complex Bruno function. Our aim is to show its relation with the nearest integer continued fraction: For this reason, we call it *1/2-Monoid*. We will prove that given  $p/q \in [0, 1)$  we can “fill” the matrix  $g_* = \begin{pmatrix} p & p \\ q_* & q \end{pmatrix}$  in exactly two ways, such that it belongs to  $\hat{\mathcal{M}}$  “following the nearest integer continued fraction development.”

**Proposition 2.7.** *Let  $p/q \in [0, 1)$ ,  $\bar{n} \geq 1$ , and assume  $p/q = [(a_0, \varepsilon_0), \dots, (a_{\bar{n}}, \varepsilon_{\bar{n}})]$  to be the finite continued fraction of  $p/q$ . We claim that the matrices  $g_T = \begin{pmatrix} p_T & p \\ q_T & q \end{pmatrix}$  and  $g_S = \begin{pmatrix} p_S & p \\ q_S & q \end{pmatrix}$ , where the rational  $p_T/q_T$  and  $p_S/q_S$  have been defined in Proposition 2.6, are given by*

$$g_T = \hat{\varepsilon}_0 g(\hat{a}_1) \dots g(\hat{a}_{\bar{n}-1}) \hat{\varepsilon}_{\bar{n}-1} g(a_{\bar{n}}) \quad (\text{Type T}) \quad (2-21)$$

$$g_S = \hat{\varepsilon}_0 g(\hat{a}_1) \dots g(\hat{a}_{\bar{n}-1}) \hat{\varepsilon}_{\bar{n}-1} g(a_{\bar{n}} - 1) g(1) \quad (\text{Type S}), \quad (2-22)$$

where for  $i = 0, \dots, \bar{n} - 1$ , matrices  $\hat{\varepsilon}_i$  and integer  $\hat{a}_i$  are defined by

$$(\hat{a}_i, \hat{\varepsilon}_i) = \begin{cases} (a_i, 1) & \text{if } \varepsilon_i = +1 \\ (a_i - 1, \sigma) & \text{if } \varepsilon_i = -1 \end{cases}. \quad (2-23)$$

Before proving the proposition, we make the following remark:

**Remark 2.8.** For all  $i$ ,  $\hat{a}_i \geq 2$ , in fact, whenever  $\varepsilon_i = -1$  one has  $a_i \geq 3$  (see Remark 2.2). Because  $p/q \in [0, 1)$ , the first couple  $(a_0, \varepsilon_0)$  can only be one of the following two:  $(0, +1)$  if  $p/q \in [0, 1/2]$  or  $(1, -1)$  if  $p/q \in (1/2, 1)$ .

*Proof:* Let  $k \leq \bar{n}$  and let us introduce matrices  $\hat{\varepsilon}_0, \dots, \hat{\varepsilon}_{k-1}$  and integers  $\hat{a}_0, \dots, \hat{a}_k$  as in (2-23) according to the continued fraction of  $p/q$ . Then we claim that  $g = \hat{\varepsilon}_0 g(\hat{a}_1) \dots g(\hat{a}_{k-1}) \hat{\varepsilon}_{k-1} g(a_k)$  is equal to  $\begin{pmatrix} p_{k-1} & p_k \\ q_{k-1} & q_k \end{pmatrix}$  where  $p_k/q_k = [(a_0, \varepsilon_0), \dots, (a_k, \varepsilon_k)]$ . This can be proved by induction (use Remark 2.8 to prove the basis of induction) and then (2-21) follows by putting  $k = \bar{n}$ . To prove (2-22), it is enough to calculate

$$\begin{aligned} &\hat{\varepsilon}_0 g(\hat{a}_1) \dots g(\hat{a}_{k-1}) \hat{\varepsilon}_{k-1} g(a_k - 1) g(1) = \\ &\begin{pmatrix} p_{k-1} & p_k - p_{k-1} \\ q_{k-1} & q_k - q_{k-1} \end{pmatrix} \begin{pmatrix} 0 & 1 \\ 1 & 1 \end{pmatrix} = \begin{pmatrix} p_k - p_{k-1} & p_k \\ q_k - q_{k-1} & q_k \end{pmatrix}. \end{aligned} \quad \square$$

**Remark 2.9.** Clearly matrices of type T belong to  $\hat{\mathcal{M}}$  (because  $a_{\bar{n}} \geq 2$ ), whereas those of type S belong to the monoid if and only if the continued fraction of the rational  $p/q$  ends with a couple  $(a_{\bar{n}}, \varepsilon_{\bar{n}}) = (2, 1)$ ; in fact, in this way, the matrix  $g_S$  is given by  $\hat{\varepsilon}_0 g(\hat{a}_1) \dots g(\hat{a}_{\bar{n}-1}) g(1) g(1) = \hat{\varepsilon}_0 g(\hat{a}_1) \dots g(\hat{a}_{\bar{n}-1}) \sigma g(2)$ , where we used the fact that  $\varepsilon_{\bar{n}-1} = 1$  (because  $a_{\bar{n}} = 2$ ) and  $\sigma g(m) = g(m - 1) g(1)$  for all  $m \geq 2$ .

Remark also that, if  $g$  is of type T, then it cannot end with  $\sigma g(2)$ ; in fact, this will imply a continued fraction ending with  $[\dots, (a_{\bar{n}-1}, -1), (2, 1)]$ , but we know that this is impossible and so either  $\varepsilon_{\bar{n}-1} = -1$ ,  $a_{\bar{n}} \geq 3$  and  $g_T = \dots \sigma g(a_{\bar{n}})$ , or  $\varepsilon_{\bar{n}-1} = +1$ ,  $a_{\bar{n}} \geq 2$ , and  $g_T = \dots g(a_{\bar{n}-1}) g(a_{\bar{n}})$ .

With the following proposition, we will prove that  $\hat{\mathcal{M}}$  is the union of matrices of type T and of type S with  $(a_{\bar{n}}, \varepsilon_{\bar{n}}) = (2, 1)$ . Let us denote by  $\mathcal{M}_T$  the monoid of matrices of type T and by  $\mathcal{M}_S$  those of type S, with  $(a_{\bar{n}}, \varepsilon_{\bar{n}}) = (2, 1)$ .

**Proposition 2.10. (The 1/2-Monoid.)**  $\hat{\mathcal{M}} = \mathcal{M}_T \cup \mathcal{M}_S$ .

*Proof:* Clearly,  $\mathcal{M}_T \cup \mathcal{M}_S \subset \hat{\mathcal{M}}$ . Let us prove the other inclusion. Let  $r \geq 1$ ,  $m_1, \dots, m_r \geq 2$ ,  $\hat{\varepsilon}_0, \dots, \hat{\varepsilon}_{r-1} \in \{1, \sigma\}$ , such that  $g = \hat{\varepsilon}_0 g(m_1) \dots \hat{\varepsilon}_{r-1} g(m_r) \in \hat{\mathcal{M}}$ .

Let us consider two cases: first,  $\hat{\varepsilon}_{r-1} = \sigma$  and  $m_r \geq 3$  or  $\hat{\varepsilon}_{r-1} = 1$  and  $m_r \geq 2$ ; second,  $\hat{\varepsilon}_{r-1} = \sigma$  and  $m_r = 2$ . In the former case, we associate a continued fraction to  $g$  by introducing, for  $i = 1, \dots, r - 1$

$$\begin{aligned} (a_0, \varepsilon_0) &= \begin{cases} (0, +1) & \text{if } \hat{\varepsilon}_i = 1 \\ (1, -1) & \text{if } \hat{\varepsilon}_i = \sigma \end{cases} \\ (a_i, \varepsilon_i) &= \begin{cases} (m_i, +1) & \text{if } \hat{\varepsilon}_i = 1 \\ (m_i + 1, -1) & \text{if } \hat{\varepsilon}_i = \sigma \end{cases} \\ a_r &= m_r. \end{aligned}$$

$[(a_0, \varepsilon_0), \dots, (a_r, \varepsilon_r)]$  represents some rational  $p/q$ ; let us define as before  $p_T/q_T$  and then  $g_T = \begin{pmatrix} p_T & p \\ q_T & q \end{pmatrix} = \hat{\varepsilon}_0 g(\hat{a}_1) \dots \hat{\varepsilon}_{r-1} g(\hat{a}_r)$  (by Proposition 2.7, where we also defined  $\hat{a}_i$ ). Observe that  $\hat{a}_i = m_i$  to conclude  $g = g_T \in \mathcal{M}_T$ .

The second case can be treated similarly. Now we associate to  $g$  the continued fraction  $[(a_0, \varepsilon_0), \dots, (a_{r-1}, 1), (2, 1)]$  where, for  $i = 1, \dots, r - 2$ :

$$\begin{aligned} (a_0, \varepsilon_0) &= \begin{cases} (0, +1) & \text{if } \hat{\varepsilon}_i = 1 \\ (1, -1) & \text{if } \hat{\varepsilon}_i = \sigma \end{cases} \\ (a_i, \varepsilon_i) &= \begin{cases} (m_i, +1) & \text{if } \hat{\varepsilon}_i = 1 \\ (m_i + 1, -1) & \text{if } \hat{\varepsilon}_i = \sigma \end{cases} \\ a_{r-1} &= m_{r-1}. \end{aligned}$$

Let  $[(a_0, \varepsilon_0), \dots, (a_{r-1}, 1), (2, 1)]$  be some rational  $p/q$ ; define as before  $p_S/q_S = [(a_0, \varepsilon_0), \dots, (a_{r-1}, 1), (1, 1)]$ , then by Proposition 2.7,

$$\begin{aligned} g_S &= \hat{\varepsilon}_0 g(\hat{a}_1) \dots g(\hat{a}_{r-1}) g(1) g(1) \\ &= \hat{\varepsilon}_0 g(\hat{a}_1) \dots g(\hat{a}_{r-1}) \sigma g(2) \\ &= g \end{aligned}$$

and it belongs to  $\mathcal{M}_S$ . □

To end this section, we introduce a third characterization of the 1/2-Monoid, which corrects a small error in Section A.4.4, page 836 of [Marmi et al. 01], and which will be useful to construct the numerical algorithm for the 1/2-complex Bruno function.

**Proposition 2.11.** Let  $g = \begin{pmatrix} a & b \\ c & d \end{pmatrix} \in G$ . Then  $g$  belongs to  $\hat{\mathcal{M}}$  if and only if  $d \geq b > 0$ ,  $c \geq a \geq 0$ , and  $d \geq \mathcal{G}c$ , where  $\mathcal{G} = (\sqrt{5} + 1)/2$ .

The proof can be done by direct computation and we omit it. We end this part with the following remark:

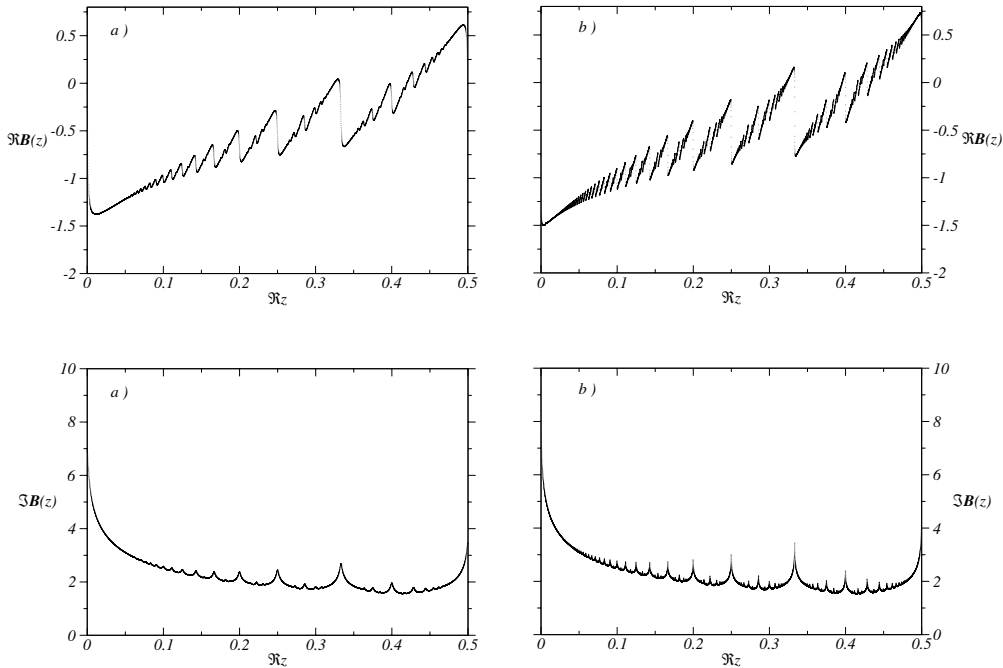


**FIGURE 1.** Plot of  $\mathbf{B}(z)$  vs  $\Re z$  at  $\Im z$  fixed. The top line contains  $\Re \mathbf{B}$  whereas on the bottom line we plot  $\Im \mathbf{B}$ . a) is for  $\Im z = 10^{-3}$ , whereas b) is for  $\Im z = 10^{-4}$ . Each plot has 10000 points  $\Re z$  uniformly distributed in  $[0, 1/2]$ .  $k_1 = 80$ ,  $k_2 = 20$ ,  $N_{max} = 151$ .

**Remark 2.12. (The Gauss Monoid.)** In [Marmi et al. 01], the authors considered the complex Bruno function constructed using the Monoid  $\mathcal{M}$ :

$$\mathcal{M} = \left\{ g = \begin{pmatrix} a & b \\ c & d \end{pmatrix} \in G : d \geq b \geq a \geq 0 \text{ and } d \geq c \geq a \right\}.$$

We recall that according to the Gauss continued fraction algorithm, we always have  $\varepsilon_l = +1$ ; we can then prove modified versions of Propositions 2.6 and 2.7 to conclude that  $\mathcal{M}$  is constructed “following” the Gauss continued fraction algorithm: Starting from  $p/q \in (0, 1)$ , we complete the matrix  $g_* = \begin{pmatrix} p_* & p \\ q_* & q \end{pmatrix}$  into  $g_S$  and  $g_T$ , where  $p_S/q_S$  and  $p_T/q_T$  are obtained with the Truncate and Subtract operations acting on the Gauss finite continued fraction of  $p/q$ .

**2.4 An Algorithm for the 1/2-Complex Bruno Function**

Using the results of the previous sections, we are now able to give an algorithm to compute the 1/2-Complex Bruno function. Let us rewrite definition (2–10) as

$$\mathbf{B}(z) = \sum_{n \in \mathbb{Z}} \left[ \sum_{g \in \hat{\mathcal{M}}} L_g (1 + L_\sigma) \right] \varphi_{1/2}(z - n),$$

where  $\varphi_{1/2}(z) = -\frac{1}{\pi} Li_2\left(\frac{1}{2z}\right) + \frac{1}{\pi} \log 2 \log\left(1 - \frac{1}{2z}\right)$  and the action  $L_g$  has been defined in (2–6). From the previous sections, we know that the sum over  $\hat{\mathcal{M}}$  can be replaced by a sum over  $p/q \in [0, 1)$ ,  $(p, q) = 1$ , in such a way that to each  $p/q$  we associate the matrix  $g_T$ , and also  $g_S$  whenever the continued fraction of  $p/q$  ends with  $(a_{\bar{n}}, \varepsilon_{\bar{n}}) = (2, +1)$ .

Using the periodicity and the parity properties of  $\mathbf{B}$ , we can restrict to  $\Re z \in [0, 1/2]$ . Let us consider the contribution of some  $p/q \in [0, 1)$  to  $\mathbf{B}$ . Because of the form of  $\varphi_{1/2}$  and of the action  $L_g$ , we remark that the larger is the denominator of the fraction, the smaller is its contribution to the sum; moreover, different rational numbers with the same denominator give comparable contributions, so we decide to order the rationals w.r.t. increasing denominators, in other words, according to the Farey Series. A similar statement holds w.r.t. the sum over  $\mathbb{Z}$ : Large  $n$  give small contributions to the sum. We then introduce two cutoffs to effectively compute (2–10):  $N_{max}$  denoting the largest order of the Farey Series considered and  $k_1$  the largest (in modulus)  $n \in \mathbb{Z}$  which contributes to the sum over integers.<sup>9</sup>

<sup>9</sup>For technical reasons, we prefer to introduce a third cutoff,  $k_2$ . We refer to Appendix 5.2 to explain the role of this cutoff.

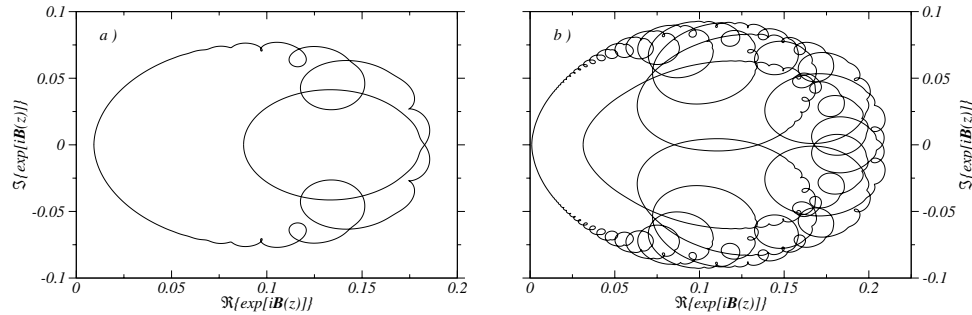


**FIGURE 2.** Polar plot of  $e^{i\mathbf{B}(z)}$  for fixed values of  $\Im z$ . a)  $\Im z = 10^{-2}$  and b)  $\Im z = 10^{-3}$ . 12000 points uniformly distributed in  $[0, 1]$ ,  $k_1 = 80$ ,  $k_2 = 20$ ,  $N_{max} = 151$ .

Then the  $1/2$ -complex Bruno function can be numerically approximated by

$$\mathbf{B}(z) \sim \sum_{|n| \leq k_1} \sum_{p/q \in \mathcal{F}_{N_{max}}} L_{\left(\frac{p_*}{q_*} \frac{p}{q}\right)} (1 + L_\sigma) \varphi_{1/2}(z - n), \tag{2-24}$$

where  $p_*/q_* \in \{p_T/q_T, p_S/q_S\}$  and the sum is restricted to fractions such that  $q \geq \mathcal{G}_{q_S}$  (where  $q \geq \mathcal{G}_{q_T}$ ). This approximation can be made as precise as we want, by choosing  $N_{max}$  and  $k_1$  large enough; in fact, (2-10) can be obtained as the double limit  $N_{max} \rightarrow +\infty$  and  $k_1 \rightarrow +\infty$ . In Appendix 5.2, we will give numerical results showing the convergence of (2-24) varying the cutoff values, the convergence of  $\Im \mathbf{B}(z)$  to  $B(\Re z)$  when  $\Im z \rightarrow 0$  and  $\Re z \in \mathcal{B}$ , and the  $\pi/q$ -jumps of  $\Re \mathbf{B}(z)$  when  $z \rightarrow p/q$ , as proved in [Marmi et al. 01]. In Figure 1, we show some plots of  $\mathbf{B}(z)$  for fixed (small) values of  $\Im z$  and  $\Re z \in [0, 1/2]$ , whereas in Figure 2 we show two polar plots of  $e^{i\mathbf{B}(z)}$ .

### 3. THE YOCOZ FUNCTION

The aim of this section is to briefly introduce the algorithm used to compute the Yoccoz Function,  $U(\lambda)$ , introduced in Section 1.1. Let  $\lambda \in \mathbb{D}^*$ , let  $P_\lambda(z) = \lambda z(1 - z)$  be the quadratic polynomial, and let us introduce the polynomials:  $U_n(\lambda) = \lambda^{-n} P_\lambda^{\circ n}(1/2)$ . Then we recall that the Yoccoz function is the uniform limit, over compact subsets of  $\mathbb{D}$ , of  $U_n(\lambda)$ .

From (1-3) and its original definition,  $H_\lambda(U(\lambda)) = 1/2$ , we get

$$U(\lambda) = \lambda^{-n} H_\lambda^{-1}(\lambda^n U_n(\lambda)), \tag{3-1}$$

for all integer  $n$ . Hence, to compute  $U(\lambda)$ , we need to know how close  $H_\lambda^{-1}$  is to the identity, near zero, and

this can be done using some standard distortion estimates [Buff et al. 01]. So for any fixed  $\lambda \in \mathbb{D}^*$ , we can find  $n = n(\lambda)$  s.t.  $P_\lambda^{\circ n}(1/2)$  is contained in some fixed disk on which we can apply the distortion estimate and then from (3-1) compute an approximation to  $U(\lambda)$  with a prescribed precision  $\epsilon_U$ .

**Remark 3.1. (Parity of Yoccoz’s Function.)** Let us observe the following facts. Assume  $\lambda = e^{2\pi i(x+it)}$ , with  $t > 0$  fixed, and  $x$  varying in  $(0, 1/2)$  and let us introduce  $u(x) = U(e^{2\pi i(x+it)})$ , to stress the dependence on  $x$  only. Then we claim that  $\Re u(-x) = \Re u(x)$  and  $\Im u(-x) = -\Im u(x)$ . The proof can be done as follows. First remark that  $\lambda$ , as a function of  $x$ , is mapped into  $\bar{\lambda}$ , when  $x \mapsto -x$ ; then it is enough to observe that polynomials  $U_n(\lambda)$  verify, for  $n \geq 2$ ,  $U_n(\bar{\lambda}) = \overline{U_n(\lambda)}$ , namely,

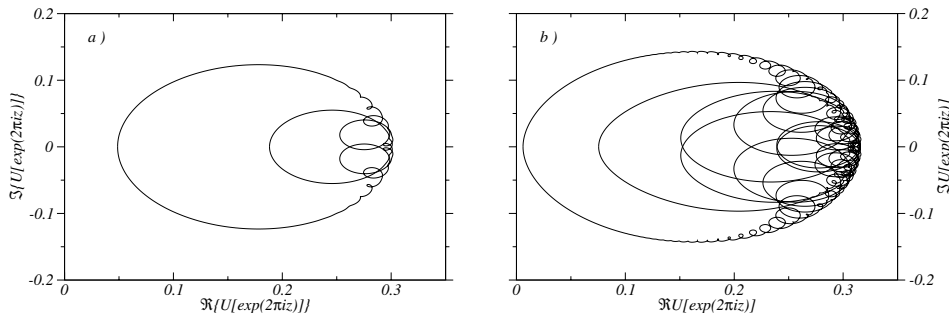
$$\begin{aligned} \Re U_n(e^{2\pi i(x+it)}) &= \Re U_n(e^{2\pi i(-x+it)}) \text{ and} \\ \Im U_n(e^{2\pi i(x+it)}) &= -\Im U_n(e^{2\pi i(-x+it)}). \end{aligned}$$

A similar statement holds for  $\log U(\lambda)$ .

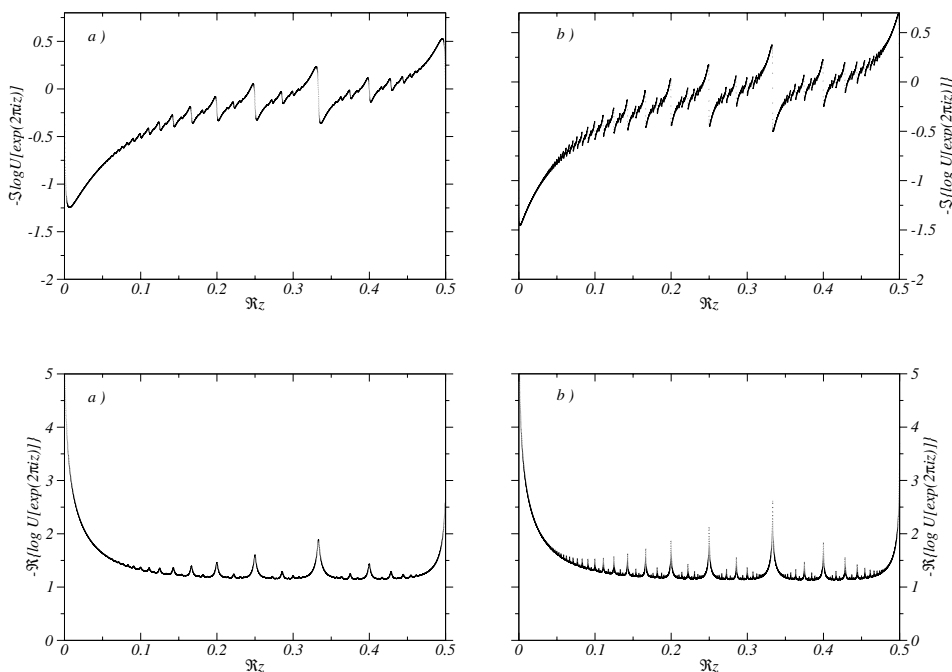
Using the  $\mathbb{Z}$ -periodicity, we consider the Fourier series of  $U(e^{2\pi iz})$  and using an argument similar to the one of Remark 2.1, we conclude that all the Fourier coefficients are real and zero for negative Fourier modes. Clearly Taylor’s coefficients of  $U(\lambda)$  coincide with Fourier coefficients of  $U(e^{2\pi iz})$ .

Figure 3 shows some polar plots of  $U(e^{2\pi iz})$ , for different values of  $\Im z > 0$ , whereas in Figure 4 real and imaginary parts of  $-\log U(e^{2\pi iz})$  are given. Compare with Figures 1 and 2.

Let us conclude this section with the following remark.



**FIGURE 3.** Polar plot of  $U(e^{2\pi iz})$  for fixed values of  $\Im z$ . a)  $\Im z = 10^{-2}$  and b)  $\Im z = 10^{-3}$ . 12000 points uniformly distributed in  $[0, 1]$ ,  $\epsilon_U = 10^{-3}$ .



**FIGURE 4.** Plot of  $-\log U(e^{2\pi iz})$  vs  $\Re z$  at fixed  $\Im z$ . On the top, we plot the imaginary part whereas on the bottom, we plot the real part. a) is for  $\Im z = 10^{-3}$ , whereas in b), we show  $\Im z = 10^{-4}$ . Each plot has 10000 points uniformly distributed in  $[0, 1/2]$ ,  $\epsilon_U = 10^{-3}$ .

**Remark 3.2.** In Figure 5, we show some polar plots of the “Yoccoz function” used in [Buff et al. 01] (Figure 2, page 484): They don’t look like our previous pictures. Here is the reason. They take the following quadratic polynomial  $Q_\lambda(z) = \lambda z + z^2$ , which can be conjugate to our choice,  $P_\lambda(z) = \lambda z(1 - z)$ , using  $\Lambda(z) = -\lambda z$ :

$$\Lambda \circ P_\lambda = Q_\lambda \circ \Lambda.$$

Let us denote by  $V(\lambda)$  the Yoccoz function for the polynomial  $Q_\lambda$ ; then we claim that:

$$-\lambda U(\lambda) = V(\lambda),$$

which explain completely the relation between Figure 3 and Figure 5. Because  $-\Im \log U(\lambda)$  exhibits the same jumps at rationals as the real part of the complex Bruno function does, we choose the quadratic polynomial in the form  $P_\lambda$ .

#### 4. THE LITTLEWOOD-PALEY THEORY

The aim of this section is to introduce the basic ideas and results of the *Littlewood-Paley Theory*; for a more com-

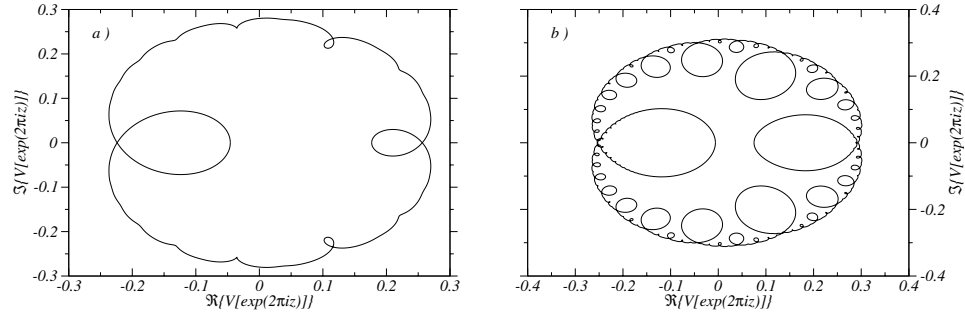


**FIGURE 5.** Polar plot of  $V(e^{2\pi iz})$  for fixed values of  $\Im z$ . a)  $\Im z = 10^{-2}$  and b)  $\Im z = 10^{-3}$ . 12000 points uniformly distributed in  $[0, 1]$ ,  $\epsilon_V = 10^{-3}$ .

plete discussion, we refer to [Stein 70, Frazier et al. 91] and also to [De la Llave and Petrov 02] where authors apply this theory to study the regularity properties of the conjugating function for *critical circle maps*. In Section 5.1, we will present the numerical implementation of this theory to study the Hölder regularity of the function  $\mathcal{H}$  and the obtained estimate for the Hölder exponent. The decay rate of the coefficients of a *Trigonometric series*,  $\sum_{\mathbb{Z}} c_k e^{2\pi i k x}$ , does not determine whether this series is the *Fourier series* of some  $L^p$  function if  $p \neq 2$ . More precisely, given  $f \in L^p$ ,  $1 \leq p < 2$  and its Fourier series  $\sum_{\mathbb{Z}} \hat{f}_k e^{2\pi i k x}$ , then for “almost every choice of signs  $\pm 1$ ,” the series  $\sum_{\mathbb{Z}} (\pm 1) \hat{f}_k e^{2\pi i k x}$  is not the Fourier series of a  $L^p$  function. This problem has been overcome by Littlewood and Paley by “grouping together” trigonometric coefficients in *dyadic blocks*. Let  $A > 1$ ,  $(\mathcal{L}_0 f)(x) = \hat{f}_0$ , and, for  $M \geq 1$ , let  $(\mathcal{L}_M f)(x) = \sum_{A^{M-1} \leq |n| < A^M} \hat{f}_n e^{2\pi i n x}$  be the *dyadic partial sum* of  $f$ . Introducing the *Littlewood-Paley d-function*,

$$d(f)(x) = \left[ \sum_{M \geq 0} |\mathcal{L}_M f(x)|^2 \right]^{1/2},$$

one can prove [Littlewood and Paley 31, Frazier et al. 91] that for all  $1 < p < +\infty$ , there exist positive constants  $A_p$  and  $B_p$  such that

$$A_p \|f\|_p \leq \|d(f)\|_p \leq B_p \|f\|_p.$$

The Littlewood-Paley Theory is indeed more general, allowing us to characterize other functional spaces by property of Fourier coefficients, for instance, it applies [Frazier et al. 91] to Sobolev spaces, Hardy spaces, Hölder spaces, and Besov spaces. In the case of Hölder regularity, one can easily realize that Fourier coefficients of an  $\eta$ -Hölder continuous function decay according to

$\hat{f}_l = \mathcal{O}(|l|^{-\eta})$ ; the converse is not true, but again the Littlewood-Paley Theory can characterize the Hölder regularity by the decay rate of the dyadic blocks.

An important tool in the theory of Fourier series is the *Poisson kernel*:  $P_s(x) = \sum_{k \in \mathbb{Z}} s^{|k|} e^{2\pi i k x}$ ,  $s \in [0, 1]$  and  $x \in \mathbb{T}$ . Let  $(f * g)(x) = \int_0^1 f(\xi)g(x - \xi) d\xi$  be the convolution product for 1-periodic functions. Then one can prove the following result ([Stein 70] Lemma 5 or [Krantz 83] Theorem 15.6)

**Theorem 4.1. (Continuous Littlewood-Paley.)** *Let  $0 < \eta < r$ ,  $r \in \mathbb{N}$ , and  $f$  be a continuous 1-periodic function. Then  $f$  is  $\eta$ -Hölder continuous if and only if there exists  $C > 0$  such that for all  $t > 0$ ,*

$$\left\| \left( \frac{\partial}{\partial t} \right)^r \mathcal{P}_f(x, t) \right\|_{\infty} \leq C t^{\eta-r},$$

where  $\mathcal{P}_f(x, t) = (P_{e^{-2\pi t}} * f)(x)$ .

We remark that if the theorem holds for some  $r \in \mathbb{N}$ , then the same is true for any  $r_1 \in \mathbb{N}$ ,  $r_1 > r$ . We call this theorem *Continuous Littlewood-Paley* to distinguish it from the following result, which is more close to the original idea of dyadic decomposition and we will call it *Discrete Littlewood-Paley* (see [Krantz 83] Theorem 5.9)

**Theorem 4.2. (Discrete Littlewood-Paley.)** *Let  $\eta > 0$  and let  $f \in C^0(\mathbb{T})$ . Then  $f$  is  $\eta$ -Hölder continuous function if and only if for all  $A > 1$  there exists a positive constant  $C$  such that for all  $M \in \mathbb{N}$ , we have*

$$\|\mathcal{L}_M f\|_{\infty} \leq C A^{-\eta M}.$$

One usually takes  $A = 2$ , and so the name dyadic decomposition, but the result is independent of the value

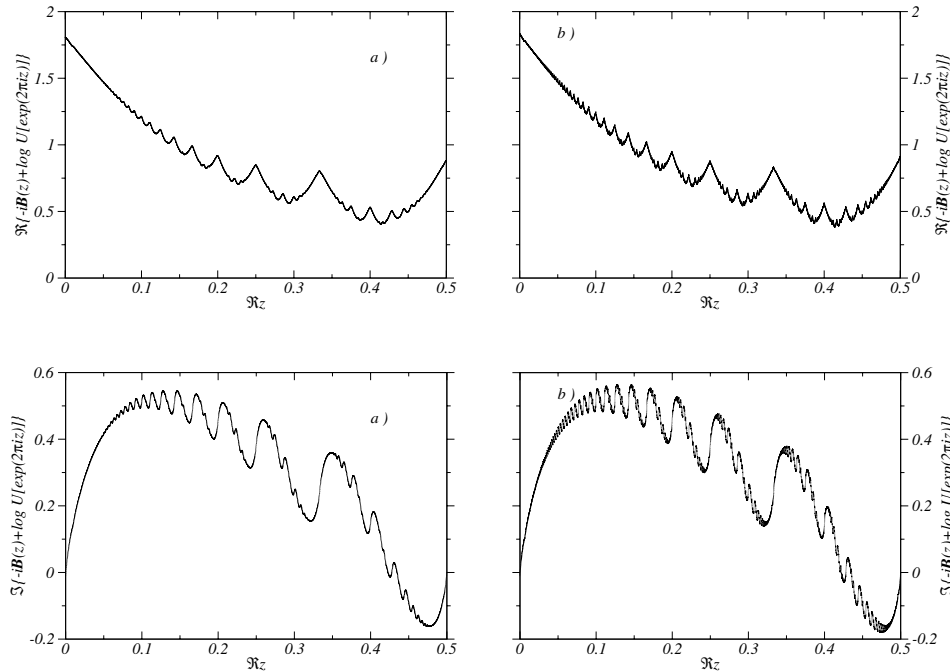


**FIGURE 6.** Plot of  $-i \mathbf{B}(z) + \log U(e^{2\pi iz})$  vs  $\Re z$  at fixed  $\Im z$ . On the top, we show the real part whereas on the bottom, we show the imaginary one. a) is for  $\Im z = 10^{-3}$  and b) for  $\Im z = 10^{-4}$ . Each plot has 10000 points uniformly distributed in  $[0, 1/2]$ .  $k_1 = 80$ ,  $k_2 = 20$ ,  $N_{max} = 151$ , and  $\epsilon_U = 10^{-3}$ .

of  $A$ . In the numerical implementation of this method, we will use a value  $A$  close to 1.25 for computational reasons.

### 5. PRESENTATION OF NUMERICAL RESULTS

This section collects our numerical results about the Marmi-Moussa-Yoccoz conjecture that we recall here: *The analytic function, defined on  $\mathbb{H}^+$ :  $z \mapsto \mathcal{H}(z) = \log U(e^{2\pi iz}) - i \mathbf{B}(z)$ , extends to a  $1/2$ -Hölder continuous function on the closure of  $\mathbb{H}^+$ .*

Let us begin with some consideration concerning  $\mathcal{H}$ . Remark 2.1 and Remark 3.1 imply that

$$\begin{aligned} \Im \mathcal{H}(x + iy) &= -\Im \mathcal{H}(-x + iy) \quad \text{and} \\ \Re \mathcal{H}(x + iy) &= \Re \mathcal{H}(-x + iy), \end{aligned}$$

for all  $y > 0$  and  $x \in [0, 1/2]$ . Moreover,  $\mathcal{H}(z)$  is 1-periodic and its Fourier series has only real coefficients, which correspond to nonnegative Fourier modes:  $\mathcal{H}(z) = \sum_{l \geq 0} \hat{h}_l e^{2\pi i l z}$ .

In Figure 6, we plot real and imaginary parts of  $\mathcal{H}(z)$  for some fixed small  $\Im z$ ; remark that  $\mathcal{H}$  still has a “structure,” but jumps of  $\mathbf{B}$  and  $-\log U$  seem to “compensate” to give a *continuous function*. The same fact holds for

the “bubbles” (using the terminology of [Buff and Chéritat 03]) of  $U(e^{2\pi iz})$  and  $e^{i \mathbf{B}(z)}$ . Figure 7 show some polar plots of  $e^{\mathcal{H}(z)}$  for fixed small  $\Im z > 0$ ; there are still some “bubbles,” but they are far from  $(0, 0)$ .

The Hölder continuity will be proved in the next paragraph, by giving an estimate of the Hölder exponent applying the *Littlewood-Paley Theory* in the *Discrete* and *Continuous* versions.

#### 5.1 Numerical Littlewood-Paley Method

To numerically implement the Littlewood-Paley Theory, we compute from the numerical values of  $\mathcal{H}$  a finite, but large, number of Fourier coefficients. Then to apply Theorem 4.1, we remark that the convolution with the Poisson Kernel and the  $r$ th derivative has the form:

$$\left(\frac{\partial}{\partial t}\right)^r (P_{exp(-2\pi t)} * \mathcal{H})(x) = \sum_{l \geq 0} (-2\pi l)^r e^{-2\pi t l} \hat{h}_l e^{2\pi i l x},$$

where we used the previous remark on the Fourier coefficients of  $\mathcal{H}$ .

We numerically compute  $\left\| \left(\frac{\partial}{\partial t}\right)^r (P_{exp(-2\pi t)} * \mathcal{H}) \right\|_\infty$  for several small values of  $t$  and some  $r > 1$ ; then applying

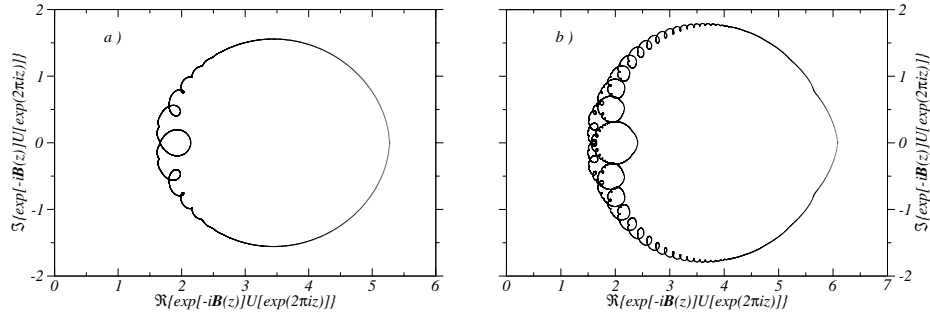


**FIGURE 7.** Polar plot of  $e^{-iB(z)}U(e^{2\pi iz})$  for fixed values of  $\Im z$ . a)  $\Im z = 10^{-2}$  and b)  $\Im z = 10^{-3}$ . 12000 points uniformly distributed in  $[0, 1]$ ,  $k_1 = 80$ ,  $k_2 = 20$ ,  $N_m = 101$ ,  $\epsilon_U = 10^{-3}$ .

a linear regression over the data,

$$\log \left\| \left( \frac{\partial}{\partial t} \right)^r (P_{exp(-2\pi t)} * \mathcal{H}) \right\|_{\infty} = C'_r - \beta_{CLP}(r) \log t, \tag{5-1}$$

we obtain a numerical value for  $\eta_{CLP}^{(r)} = r - \beta_{CLP}(r)$ .

From a numerical point of view, the continuous version of the Littlewood-Paley method is better than the discrete one; in fact, the former has two parameters to vary  $t$  and  $r$ . We can vary  $r$  to control whether the computed value of  $\eta_{CLP}^{(r)}$  stays constant or not. Moreover, we can compute the l.h.s. of (5-1) for many values of  $t$  and for each one, all the known Fourier coefficients are used, whereas in the dyadic decomposition to “small”  $M$  only, “few” Fourier coefficients give their contribution and only for “large”  $M$  a large number of Fourier coefficients enter.

In Figure 8, we report data from (5-1) and the corresponding linear regression values.<sup>10</sup> The estimated values of  $\eta$  obtained for different  $r$  are  $\eta_{CLP}^{(r=2)} = 0.497 \pm 0.003$ ,  $\eta_{CLP}^{(r=3)} = 0.498 \pm 0.004$ , and  $\eta_{CLP}^{(r=4)} = 0.498 \pm 0.003$  (errors are standard deviation errors of linear regression). They agree in the numerical precision and this gives a good indication of the validity of the results. There is no reason to prefer one value to the other and so we estimate  $\eta_{CLP} = 0.498 \pm 0.004$ : the mean value of the interval obtained by the union of the three intervals obtained for  $r = 2, 3, 4$ .

We also report the numerical results obtained using the discrete Littlewood-Paley Theorem. We fix some  $A > 1$ <sup>11</sup> and from the computed Fourier coefficients of  $\mathcal{H}$  we construct the dyadic partial sums for some large

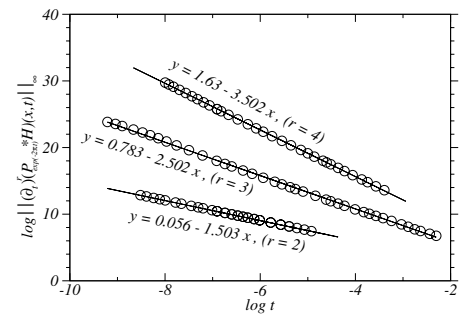


**FIGURE 8.** The function  $\log t \mapsto \log \left\| \left( \frac{\partial}{\partial t} \right)^r \mathcal{P}_{\mathcal{H}}(x, t) \right\|_{\infty}$ , for  $r = 2$ ,  $r = 3$ , and  $r = 4$ . We also show the linear regressions (5-1).

$M \in \mathbb{N}$ . Then we use a linear regression on the data,

$$\log_A \|\mathcal{L}_M f\|_{\infty} = C_{DLP} - \eta_{DLP} M, \tag{5-2}$$

to obtain the estimate value of the Hölder coefficient:  $\eta_{DLP} = 0.50 \pm 0.03$  and  $C_{DLP} = -4.90 \pm 0.66$ . In Figure 9, we report data from (5-2) and the linear regression applied on “large  $M$ .”

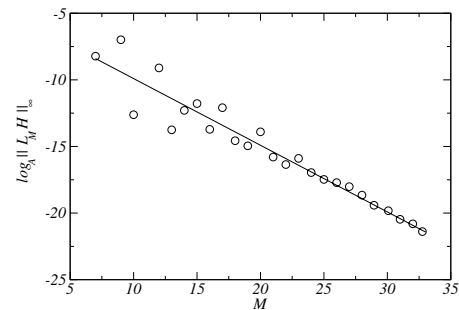


**FIGURE 9.** The function  $M \mapsto \log_A \|\mathcal{L}_M \mathcal{H}\|_{\infty}$  and the linear fit  $\log_A \|\mathcal{L}_M \mathcal{H}\|_{\infty} = C_{DLP} - \eta_{DLP} M$ .

<sup>10</sup>In the figure, we decided to show only few points to have an “intelligible picture,” but the linear regression is made using hundreds of points.

<sup>11</sup>The exact value of  $A$  is fixed in such a way that we can take  $M$  sufficiently large to have a good asymptotic, even if we have a finite number of Fourier coefficients.

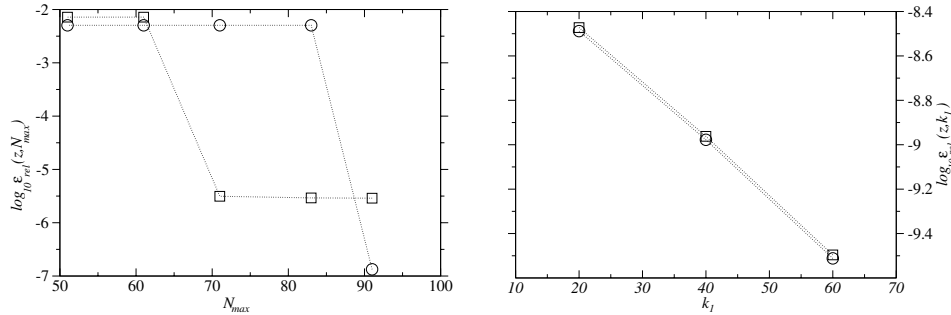


FIGURE 10. Plot of  $\log_{10} \epsilon_{rel}(z, M)$  for some “good”  $z$ . On the left we show  $\log_{10} \epsilon_{rel}(z, N_{max})$  whereas on the right  $\log_{10} \epsilon_{rel}(z, k_1)$ . Circles are for  $z = 2 - \mathcal{G} + i10^{-7}$  and squares are for  $z = \sqrt{2} - 1 + i10^{-7}$ .

5.2 Conclusion

We conclude this paper by summarizing the obtained results. We introduced the 1/2-complex Bruno function and the Yoccoz function, both with an algorithm to evaluate them numerically. We studied the function  $\mathcal{H}(z) = -i\mathbf{B}(z) + \log U(e^{2\pi iz})$  defined on the upper Poincaré plane, and we gave numerical evidence that it can be extended to its closure, with a trace  $\eta$ -Hölder continuous. Numerical results based on the Littlewood-Paley Theory give us the estimated value for the Hölder exponent:  $\eta_{CLP} = 0.498$  with an error of  $\pm 0.004$ . We can then conclude, with a good numerical evidence, that the Marmi-Moussa-Yoccoz Conjecture should hold with the maximal exponent 1/2.

APPENDIX A. NUMERICAL CONSIDERATIONS

The aim of this appendix is to consider in detail some technical parts of our numerical calculations. We will consider the role of the cutoff and its relation to the accuracy of the computations. We will also compare the numerical properties of  $\mathbf{B}$  with the analytical ones proved in [Marmi et al. 01].

A.1 Accuracy of the Algorithm for  $\mathbf{B}(z)$

Let us recall the formula defining the 1/2-complex Bruno function:

$$\mathbf{B}(z) = \sum_{n \in \mathbb{Z}} \left[ \sum_{g \in \mathcal{M}} L_g (1 + L_\sigma) \right] \varphi_{1/2}(z - n);$$

as already observed, we need to introduce three cutoffs to compute it:  $N_{max}$ ,  $k_1$  and  $k_2$ . The first one determines the largest Farey Series involved; namely only fractions  $p/q$  s.t.  $p/q \in [0, 1)$ ,  $(p, q) = 1$ , and  $q \leq N_{max}$  will

be considered to compute  $\mathbf{B}$ . The other two cutoffs,  $k_1 \geq k_2 > 0$ , are introduced to truncate the sum over  $\mathbb{Z}$ . Because the larger  $q$  is, the smaller is its contribution to  $\mathbf{B}$ , to gain CPU times, we decide to truncate the sum over  $\mathbb{Z}$  at  $|n| \leq k_1$  if  $q$  is “small,” and to  $|n| \leq k_2$  if  $q$  is “large.” Results showed in Section 5. are obtained with  $N_{max} = 151$ ,  $k_1 = 80$ , and  $k_2 = 20$ .

In the rest of this paragraph, we will study the dependence of the computed Bruno function on the cutoff. Let us fix all except one cutoff, call it generically  $M$ , and stress the dependence of  $\mathbf{B}$  on it by setting  $\mathbf{B}_M(z)$ . We are then interested in studying the relative error:  $\epsilon_{rel}(z, M) = |\mathbf{B}_M(z) - \mathbf{B}(z)|/|\mathbf{B}(z)|$ , where  $z$  is fixed and  $\mathbf{B}(z)$  is numerically computed with some fixed large cutoff:  $N_{max} = 101$ ,  $k_1 = 80$ , and  $k_2 = 20$ . Or we can consider  $\bar{\epsilon}_{rel}(M)$  the mean value of  $\epsilon_{rel}(z, M)$  for  $\Re z \in [0, 1/2]$  and some fixed value of  $\Im z > 0$ . In Table 1, we report values of  $\log_{10} \bar{\epsilon}_{rel}(M)$ , for  $M \in \{N_{max}, k_1, k_2\}$ ; in Figure 10 we show  $\log_{10} \epsilon_{rel}(z, M)$ , for  $M = N_{max}$  and  $M = k_1$  and  $z \in \{\sqrt{2} - 1, 2 - \mathcal{G}\}$ . Clearly the larger the cutoffs, the more accurate the results, but recall that large cutoffs imply large CPU times; in particular, the CPU times increase almost linearly w.r.t.  $k_1$  and  $k_2$ , but quadratically w.r.t.  $N_{max}$ .

$N_{qmax}$	$\log_{10} \bar{\epsilon}_{rel}(N_{max})$	$k_1$	$\log_{10} \bar{\epsilon}_{rel}(k_1)$	$k_2$	$\log_{10} \bar{\epsilon}_{rel}(k_2)$
83	-5.90	60	-9.57	15	-10.80
61	-4.73	40	-9.10	10	-10.32
41	-3.81	20	-8.63		

TABLE 1. We report  $\log_{10} \bar{\epsilon}_{rel}(N_{max})$ ,  $\log_{10} \bar{\epsilon}_{rel}(k_1)$ , and  $\log_{10} \bar{\epsilon}_{rel}(k_2)$ .

To have a full test of our algorithm, we try to evaluate the limit, for  $\Im z \rightarrow 0$ , of the computed  $\mathbf{B}$  and compare it with the results proved in [Marmi et al. 01]: Section 5.2.9, page 816 and Theorem 5.19, page 827. In partic-

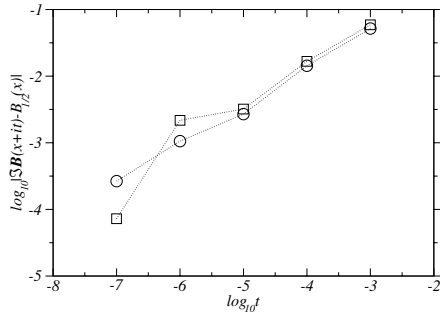


**FIGURE 11.** Convergence of  $\Im \mathbf{B}(x + it)$  to  $B_{1/2}(x)$  when  $t \rightarrow 0$  for some “good irrational”  $x$ . Circles are for  $x = 2 - \mathcal{G}$  whereas squares are for  $x = \sqrt{2} - 1$ . We plot  $\log_{10}|\Im \mathbf{B}(x + it) - B_{1/2}(x)|$  versus  $\log_{10} t$ .  $N_{qmax} = 101$ ,  $k_1 = 80$ , and  $k_2 = 20$ .

ular, we will be interested in studying the rate of convergence of  $\Im \mathbf{B}(x + it)$  to  $B_{1/2}(x)$ , for  $t \rightarrow 0$  when  $x$  is some “good” number (Figure 11), and the “jump value” of  $\Re \mathbf{B}(p/q + it)$ , when  $t$  is “small” (Table 2).

$p/q$	$\Delta \Re \mathbf{B}(p/q + it) - \pi/q$
0/1	$1.1 \cdot 10^{-3}$
1/2	$7.4 \cdot 10^{-4}$
1/3	$3.6 \cdot 10^{-3}$
1/4	$3.6 \cdot 10^{-3}$
1/5	$3.8 \cdot 10^{-3}$
2/5	$2.5 \cdot 10^{-3}$

**TABLE 2.** The jumps of  $\Re \mathbf{B}(x + it)$  for rational  $x$  and small  $t$ . The jump at  $x = p/q$  is the numerical difference  $|\Re \mathbf{B}(p/q + \delta + it) - \Re \mathbf{B}(p/q - \delta + it)|$ , for  $\delta$  small. We report the difference of the jump w.r.t the expected value for  $x \in \{0/1, 1/2, 1/3, 1/4, 1/5, 2/5\}$  and  $t = 10^{-7}$ .

**ACKNOWLEDGMENTS**

I am grateful to Jacques Laskar for putting at my disposal a large amount of CPU time on computers of the *Astronomie et Systèmes Dynamiques* Team at IMCCE Paris.

**REFERENCES**

[Berretti and Gentile 01] A. Berretti and G. Gentile. “Bryuno Function and the Standard Map.” *Comm. Math. Phys.* 220:4 (2001), 623–656.  
 [Buff et al. 01] X. Buff, C. Henriksen, and J. H. Hubbard. “Farey Curves.” *Experimental Mathematics* 10:4 (2001), 481–486.

[Buff and Cheritat 03] X. Buff and A. Cheritat. “Upper Bound for the Size of Quadratic Siegel Disks.” *Invent. Math.* (2003), DOI:10.1007/s00222-003-0331-6 (published first online).  
 [Buff and Cheritat 04] X. Buff and A. Cheritat. “The Brjuno Function Continuously Estimates the Size of Quadratic Siegel Disks.” Preprint, arXiv:math.DS/0401044 v1.  
 [Buric et al. 90] N. Buric, I. C. Percival, and F. Vivaldi. “Critical Function and Modular Smoothing.” *Nonlinearity* 3 (1990), 21–37.  
 [Carletti 03] T. Carletti. “The Lagrange Inversion Formula on Non-Archimedean Fields. Non-Analytic Form of Differential and Finite Difference Equations.” *DCDS Series A* 9:4 (2003), 835–858.  
 [Carletti and Marmi 00] T. Carletti and S. Marmi. “Linearization of Analytic and Non-Analytic Germs of Diffeomorphisms of  $(\mathbb{C}, 0)$ .” *Bull. Soc. Math. France* 128 (2000), 69–85.  
 [Davie 94] A. M. Davie. “The Critical Function for the Semi-standard Map.” *Nonlinearity* 7 (1994), 219–229.  
 [Frazier et al. 91] M. Frazier, B. Jawerth, and G. Weiss. *Littlewood-Paley Theory and the Study of Function Spaces*, Conf. Board of the Math. Sciences, 79. Providence, RI: AMS, 1991.  
 [Hardy and Wright 79] G. H. Hardy and E. M. Wright. *An Introduction to the Theory of Numbers*, Fifth edition. Oxford, UK: Oxford Univ. Press, 1979.  
 [Krantz 83] S. G. Krantz. “Lipschitz Spaces, Smoothness of Functions, and Approximation Theory.” *Exposition. Math.* 1:3 (1983), 193–260.  
 [Littlewood and Paley 31] J. E. Littlewood and R. E. A. C. Paley. “Theorems on Fourier Series and Power Series, I.” *J. London Math. Soc.* 6 (1931), 230–233.  
 [De la Llave and Petrov 02] R. de la Llave and N. P. Petrov. “Regularity of Conjugacies between Critical Circle Maps: An Experimental Study.” *Experimental Math.* 11:2 (2002), 219–241.  
 [Marmi 90] S. Marmi. “Critical Functions for Complex Analytic Maps.” *J. Phys. A: Math. Gen.* 23 (1990), 3447–3474.  
 [Marmi et al. 97] S. Marmi, P. Moussa, and J. -C. Yoccoz. “The Brjuno Functions and their Regularity Properties.” *Communications in Mathematical Physics* 186 (1997), 265–293.  
 [Marmi et al. 01] S. Marmi, P. Moussa, and J. -C. Yoccoz. “Complex Brjuno Functions.” *Journal of AMS* 14:4 (2001), 783–841.  
 [Nakada 80] H. Nakada. “On the Invariant Measures and the Entropies for Continued Fraction Transformations.” *Keio Math. Rep.* 5 (1980), 37–44.  
 [Oesterlé 93] J. Oesterlé. “Polylogarithmes, Séminaire Bourbaki n. 762.” *Astérisque* 216 (1993), 49–67.  
 [Stein 70] E. M. Stein. *Singular Integrals and Differentiability Properties of Functions*. Princeton, NJ: Princeton University Press, 1970.

[Yoccoz 95] J. -C. Yoccoz. “Théorème de Siegel, polynômes quadratiques et nombres de Brjuno.” *Astérisque* 231 (1995), 3–88.

[Yoccoz 02] J. -C. Yoccoz. “Analytic Linearization of Circle Diffeomorphisms.” In *Dynamical Systems and Small Divisors*, pp. 125–174, Lecture Notes in Mathematics 1784. Berlin: Springer-Verlag, 2002.

Timoteo Carletti, Scuola Normale Superiore, piazza dei Cavalieri 7, 56126 Pisa, Italy (t.carletti@sns.it)

Received June 3, 2003; accepted in revised form September 11, 2003.